JOURNAL DE PHYSIQUE
Colloque C3, supplément au n°3, Tome 46, mars 1985

MAGNETIC-FIELD-INDUCED ALIGNMENT AND INSTABILITIES IN ORDERED COLLOIDS OF TOBACCO MOSAIC VIRUS

S. Fraden[+], A.J. Hurd[+], R.B. Meyer[+], M. Cahoon[*] and D.L.D. Caspar[*]

[+]*Martin Fisher School of Physics*
[*]*The Rosenstiel Basic Medical Sciences Research Center*
Brandeis University, Waltham, Massachusetts 02254, U.S.A.

Résumé - Nous utilisons des champs magnétiques pour orienter des cristaux liquides nématiques ainsi que des solutions cristallines colloïdales monodisperses de virus du tabac (TMV). Les instabilités hydrodynamiques induites par les réorientations sous champ magnétique ont été étudiées sur des cristaux liquides nématiques bien orientés.

Abstract - Magnetic fields have been used to produce well aligned nematic liquid crystalline and colloidal crystalline samples of nearly monodisperse tobacco mosaic virus (TMV). Hydrodynamic instabilities induced by reorientation in a magnetic field have been studied in the well aligned nematic liquid crystalline samples.

1. INTRODUCTION

Colloidal suspensions of tobacco mosaic virus (TMV) in water have long been recognized as interesting systems for colloid science, for the study of liquid crystals, and for studies of various biophysical questions. The latter area has included studies of intermolecular forces, self assembly of ordered systems, and production of highly oriented specimens for x-ray diffraction studies of the structure of the virus particle. This paper reports advances in the preparation and handling of colloidal samples and observations of their properties in the nematic and colloidal crystalline phases which make possible a range of experiments never before undertaken. We present a detailed description of a hydrodynamic instability that occurs when TMV in the nematic phase is made to rapidly reorient by the application of a magnetic field and we report the production of well aligned colloidal crystalline TMV. After summarizing the relevant aspects of earlier studies of colloidal TMV we present our findings.

2. PHYSICAL PROPERTIES OF TMV

Tobacco mosaic virus is a rigid rod, 3000Å in length and 180Å in diameter. It is composed of 2130 identical protein subunits in a helical array wound about a hollow core. The inside of the core is wrapped with a flat ribbon of double stranded RNA. The total molecular weight of the TMV is 4×10^7 g/mole (Fig.1).[1]
The protein sub-units that compose TMV are charged; the magnitude and sign of the charge are a function of pH and ionic strength. The isoelectric point is pH 3.3 and at pH 7.0 there are 1-2 negative charges per protein sub-unit. Thus the surface charge density is of order 1 $\mu C\ cm^{-2}$ and is very similar to the surface charge density on other colloidal particles.[2]

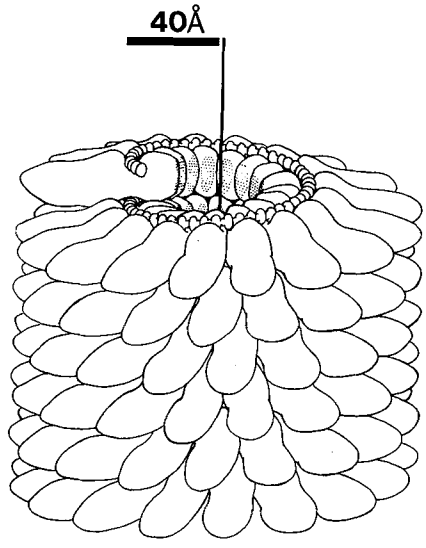

Figure 1 Tobacco mosaic virus.

Identical protein sub-units are wound about a hollow core.

A. Purification of TMV

Our studies began with virus kindly supplied by Dr. C. Wetter of the Universität des Saarlandes, Saarbrücken, Germany. Later we extracted virus from infected tobacco plants at Brandeis University using a method given to us by Dr. Wetter. The method is a combination of several preparatory procedures previously published.[3-5] End-to-end aggregation of TMV is a well known problem to people who have worked with TMV; our extraction procedures avoid aggregation by keeping the sample above pH 7.0 and below an ionic strength of 50mM salt concentration, i.e. with the particles in a highly charged, mutually repulsive state. An electron micrograph of TMV taken from our preparation is shown in Fig.2. There is a small amount of end-to-end aggregation present. One also notes the presence of fragments at least some of which are caused by the electron micrograph preparation as indicated by the fragments in registry in the upper right corner. We are currently characterizing the polydispersity with flow birefringence, sedimentation and Cotton-Mouton measurements.[6]

B. Phase Behavior of TMV

When samples are prepared as described by Kreibig and Wetter,[5] that is in low salt, highly charged conditions, the concentrated virus has a characteristic sheen due to the scattering of light. The length of the particle combined with the average separation between particles gives an average periodicity comparable to the wavelength of light, so white light is separated into colors when scattered. White light scattered from the colloidal crystalline TMV is very different from light scattered from the other phases as shown in the photographs in Ref.5: There is Bragg diffraction of light scattered from the colloidal crystalline phase that is sharply defined in scattering angle.

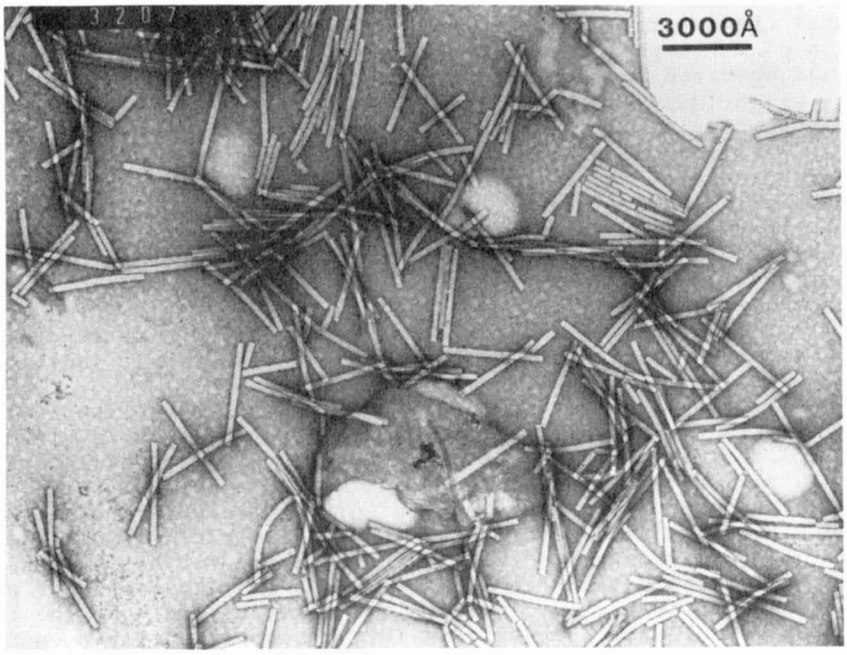

Figure 2 Electron micrograph of TMV preparation.

The thin line running down the middle of the particles is the hollow core of the virus. Note the fragments in registry in the upper right corner which indicate that the electron micrography preparation breaks the particles.

The colloidal crystalline phase has been described before but each time with different names. It was first described as an iridescent gel[7] and later as smectic layers.[5]
When the virus is diluted in water three phases are observed as a function of concentration. Specifically, our preparations in distilled water of pH 7 are isotropic at concentrations below 20 mg/ml, lyotopic nematic liquid crystalline between 20 and 30 mg/ml and colloidal crystalline above 30 mg/ml, at which concentration the slow formation of macroscopic crystals is observed.[5,7] This phase diagram is different from what most people have observed with TMV. Notably, X-ray diffraction studies have been made in samples with concentration above 300 mg/ml without observing any Bragg diffraction characteristic of crystalline ordering of the particles. We will not attempt to review the problem here but only note that the existence of the crystalline state is probably very sensitive to particle polydispersity caused by end-to-end aggregation or fragmentation of the virus and to the presence of any contaminants in the solution.

2. PREVIOUS INVESTIGATIONS OF NEMATIC AND COLLOIDAL CRYSTALLINE TMV

Tobacco mosaic virus was first extracted from infected tobacco plants in 1935[8]. Very few viruses had been isolated by that time and there was much interest in improving the quality of the extraction and puri-

fication procedure to obtain samples suitable for biochemical and structural characterization. Shortly after the first report of the isolation of TMV improvements in the extraction procedure were made and it was observed that solutions containing more than two percent virus by weight separated into two fluid phases,[9] the top phase being optically isotropic and the bottom phase birefringent. Hence TMV was recognized early on as a liquid crystal.

The observation of a liquid crystalline phase was baffling since there were no theories to explain the phase separation at such low concentrations. This provoked a number of investigations into the nature of the forces responsible for the phase separation. Measurements were made of the interparticle spacing as a function of pH and ionic strength[10] but the sample was in a so-called "gel" state which was never well characterized. There was also a brief study made to determine the concentration of virus needed to form two phases as a function of NaCl concentration at fixed pH 7.0.[11]

In 1948 Onsager[12] presented a theoretical model for the isotropic-nematic phase transition in lyotropic liquid crystals with TMV in mind as the experimental system. His theory predicts ratios of the concentrations in the co-existing isotropic and nematic phases. These ratios depend on the second virial coefficient or, equivalently, the excluded volume of the particle. Oster[7] measured the excluded volume as a function of ionic strength using light scattering but he measured the ratio of the concentrations in the two phases only at low ionic strength where the Onsager theory does not apply.[13] Oster also made the first observation of colloidal crystalline TMV, measured the layer spacing of the crystal, and made a measurement of the size of the crystallites. In 1980 Kreibig and Wetter[5] improved on Oster's work on colloidal crystalline TMV and reported an easy method of preparing iridescent virus using six different strains of tobacco-viruses. They measured the layer spacing of the crystals as a function of concentration using a high resolution light scattering apparatus and explored the temperature dependence of the spacing between layers of the crystal. They were able to show that separate crystallites had slightly different periodicities in the same local region of a sample. Their paper also contains many beautiful color photographs of the colloidal crystalline phase.

Although Onsager developed his theory of the isotropic-nematic phase transition with TMV as an example there have been no confirmations of the theory in the regime of concentration and ionic strength where the theory applies[13] nor have there been any measurements done on the liquid crystalline properties of this system. Why is this so ? Perhaps for these three reasons: First, preparation of monodisperse samples is difficult and years have been spent by many workers to establish satisfactory procedures. Second, the nematic phase exists in a narrow concentration range between the isotropic and colloidal crystalline phases and since birefringence alone does not signify a liquid crystalline state (the colloidal crystal is also birefringent), recognizing a nematic phase is not trivial. Third, oriented single domain nematic samples have never been prepared before now in a geometry suitable for a quantiative study of their liquid crystalline properties by optical and field alignment methods. We have managed to negotiate these three problems.

3. ALIGNMENT OF NEMATIC TMV

As mentioned above our sample preparations as examined by electron microscopy are nearly monodisperse. We have also been able to align the virus and produce stable single domain nematic samples using a combina-

tion of surface treatment and magnetic field alignment. Our sample cells consist of parallel plates fabricated from 0.5 inch diameter quartz windows. The TMV suspension is contained between the two quartz windows by a teflon washer of any thickness up to about a millimeter. The whole assembly is held together with a nonmagnetic clamp. The TMV particles align parallel to the glass. When the virus is initially placed in the cell the sample is somewhat misaligned. Since the virus has a positive diamagnetic anisotropy [14] which has recently been measured,[6] the particles in a nematic sample which is placed in a magnetic field align along the field direction in a reasonable time, e.g. within several minutes at a field of 22 kgauss, the maximum strength attainable with our magnet. If the sample cell is placed in the magnetic field shortly after being loaded, the alignment is usually permanent after removing the sample from the field. Often, however, the nematic remembers the initial misaligned state when taken out of the field and the sample becomes misaligned again.

We have found a surface treatment that allows the virus to lock-in to the alignment produced by the field. Uniform alignment is accomplished by using windows coated with obliquely evaporated SiO deposited with an angle of incidence of approximately 70 degrees from normal. This method of alignment is commonly used with low molecular weight liquid crystals. The SiO forms rough ridges which induce the particles to align perpendicular to the direction of incidence of the SiO. We have found that a combination of SiO-treated windows and annealing in a magnetic field is an effective way to produce uniform alignment of both colloidal crystals and nematic samples.

When viewed under the microscope with crossed polarizers, well aligned samples, which have uniform texture on the average, show faint streaks, rapidly fluctuating in time, with the streaks oriented perpendicular to the director. If we examine colloidal crystalline or end-to-end aggregated samples in this way we no longer see these characteristic anisotropic fluctuations and the samples do not respond to magnetic fields as readily. (For example, no observable reorientation occurs after several hours exposure to a 20 kgauss field.) The critical fields for the twist and splay Frederiks transitions in a typical sample (e.g.90 microns thickness and concentration 148 mg/ml at pH 8.5 in 50 mM Borate buffer) were measured as 2.2 kgauss and 3.5 kgauss respectively. These critical fields indicate the field magnitude necessary to align TMV.

4. MAGNETIC REORIENTATION INSTABILITIES

Having obtained samples that appeared to be nematic we checked to see if instabilities arose when an aligned liquid crystal sample is forced to undergo rapid reorientation in a magnetic field, an effect previously observed in lyotropic liquid crystals.[15-19] A striped texture is often observed as the initial response of an uniformly aligned nematic sample to a suddenly applied reorienting magnetic field. The instability depends on the viscoelastic anisotropy of the liquid crystal, the field strength, and in an important way on the boundary conditions imposed by the sample cell. The striped texture is transient, lasting a few seconds with thermotropics and many hours with lyotropics before uniform alignment is again obtained.

With TMV particles aligned parallel to the quartz plates, we studied in detail two geometries: one in which the field is applied normal to the director and in the plane of the sample, corresponding to the twist Frederiks transition geometry, and the other in which the field is normal to the plane of the sample, corresponding to the splay Frederiks

transition geometry. We shall refer to the former instability as the periodic twist transition whose characteristic feature is a set of parallel stripes characterized by one wave vector parallel to the initial director (Fig.3). The latter instability is the periodic splay

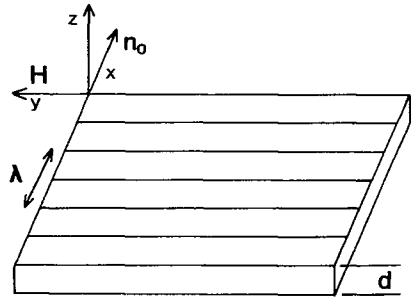

Figure 3 Geometry of the periodic twist instability.

Liquid crystal initially aligned along the x-axis is exposed to a magnetic field (H) along the y-axis. A periodic instability develops with the wave vector along the x-axis. The wavelength of the instability is λ and d is the sample thickness.

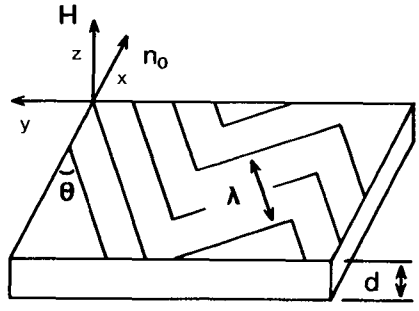

Figure 4 Geometry of the periodic splay instability.

Liquid crystal initially aligned along the x-axis is exposed to a magnetic field along the z-axis. The periodic instability is characterized by a wavelength (λ) and an angle (θ) or, equivalently, by two wave vectors $k_x = 2\pi\sin\theta/\lambda$ and $k_y = 2\pi\cos\theta/\lambda$.

transition, which produces oblique sets of stripes characterized by two wave vector components, one parallel to the initial director and one perpendicular to the initial director (Fig.4). We have presented theoretical models for the initial response of these instabilities elsewhere[20,29] and would like to take the opportunity here to describe some qualitative observations such as the full time development of these instabilities and their approach to equilibrium, which have not been described elsewhere.

A. Periodic Twist Transition

The periodic twist transition is the simplest instability to understand since the observation that the stripes are perpendicular to the original director implies that the fluid velocity and director remain in a single plane. The theory, which is presented by Lonberg et.al.[20] is based on the idea that the initial distortion is dominated by the fastest growing Fourier mode. Following Guyon, et.al.,[18] these modes are found by first solving the two-dimensional equations of nematodynamics for the rate of growth as a function of wave vector q, then finding a maximum in the growth rate by varying q.

The underlying physical causes for the appearance of a periodic distortion are the coupling between fluid flow and director rotation and the elastic and viscous anisotropy of the nematic phase. To be more specific, uniform rotation of an oriented sample as in the usual Frederiks twist transition involves a rather large purely rotational viscosity (γ_1) with no fluid flow. In the periodic distortion, however, shear viscosities become involved and tend to reduce the overall viscosity associated with reorientation. Thus alternating oppositely rotating domains are favored from a dissipation standpoint because they reduce the effective viscosity. The smaller the wavelength of the periodic distortion the smaller the effective viscosity. On the other hand large gradients in the director raise the elastic energy of the liquid crystal tending to slow down the response of short wavelength modes. The fastest growing mode achieves an optimal balance among the drag, elastic and field forces, and the elastic forces must be balanced quasistatically by the magnetic forces. Thus the wavelength of the distortion is limited by the amount of energy supplied by the external magnetic field.

An example of the periodic twist transition is shown in the illustrations of the director and velocity fields (Fig.5) and the accompanying photographs (Fig.6). The photographs show the time evolution of an instability that is nucleated at the walls. The sample is in a cell composed of parallel glass plates separated by a 400 μm thick teflon washer with a 10 mm inside diameter. As shown in the drawings the director is initially uniformly aligned except for a thin boundary layer in which it reorients to be parallel to the surface of the washer. Under crossed polarizers with the axis of the polarizer along the director, the aligned liquid crystal appears black while misaligned regions show color. The curvature of the washer breaks the symmetry of the director field into two zones, in each of which molecules near the washer are tilted in opposite directions. When the magnetic field is initially applied perpendicular to the undisturbed director the bulk of the sample is in an unstable equilibrium and does not initially respond. However, the misoriented boundary layers begin to reorient rapidly. Regions on opposite sides of the midline of the sample rotate in opposite directions. The fluid flow produced by this rotation induces counterrotation in a stripe of material next to the boundary layer near the washer. This rotation again is accelerated by the field, and in turn induces counterrotation in the stripe of material next to it. As time increases the instability propagates as a series of stripes towards the interior of the sample. It is observed that eventually alternate stripes link together across the midline of the sample. This happens because in alternate stripes on opposite sides of the midline the orientation is the same, and by linking together defects are eliminated at the midline.

The formation of stripes nucleated by the boundaries proceeds at a faster rate than the growth of stripes nucleated by thermal fluctuations far from the boundaries. This is analogous to the Rayleigh-Bénard and

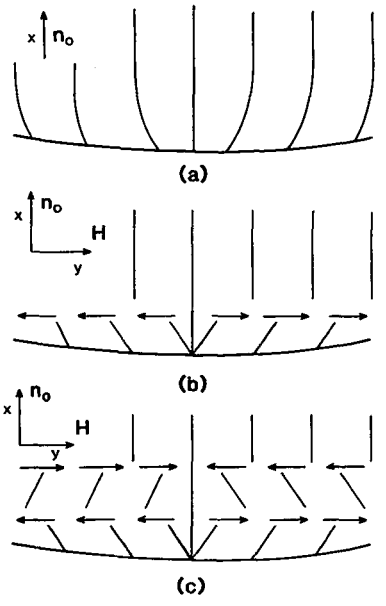

Figure 5 Temporal development of the periodic twist transition.

This sequence describes the time development of a twist instability nucleated by the boundary (see Fig. 6). (a) Director field (n) before the magnetic field is applied. (b) Initial response of the liquid crystal to a suddenly applied field along the y-axis. Arrows represent the velocity field of the fluid. (c) The instability propagates away from the boundary of the cell.

other instabilities in which both the spatial periodicity and the rate of growth of the distortion are different in the cases of homogeneous nucleation caused by thermal fluctuations and nucleation at the boundaries.[21] In the periodic twist transition we first see stripes nucleate at the boundary and propagate towards the interior of the sample, but we also observe stripes nucleating homogeneously in the center of the sample. The theory previously presented for the periodic twist transition[20] treats only the case of homogeneous nucleation, while the case of the instability nucleated by the boundary must take initial conditions into account. It may be treated by first decomposing the initial boundary layer distortion into Fourier modes and then following the time evolution of the superposition of modes to see how the total distortion increases with time.

The instability shown here develops over a period of several minutes, after which time the sample has developed well defined twist-bend walls. These walls change much less rapidly than the initial growth of the distortion. If the field is turned off before these twist-bend walls form, the sample rapidly relaxes within a minute or so to the initial alignment. If the walls are allowed to form however they take typically a half-hour to relax outisde the field to the initial alignment. In a sample of several hundred microns thickness these walls persist for about a half-hour typically in the field but finally the walls pinch in half into line disclinations of strength $\pm 1/2$. The disclinations move apart to opposite boundaries which leaves the bulk of the

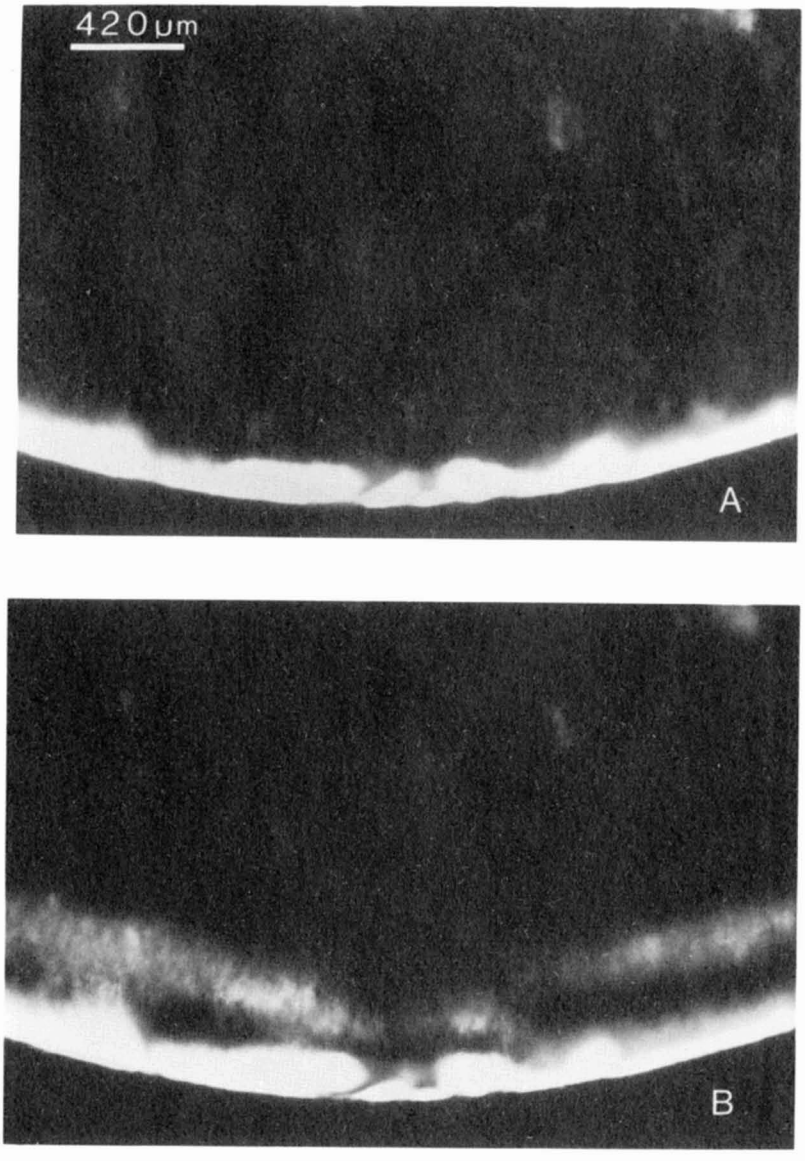

Figure 6A-B

sample aligned along the field. Once disclinations separate they can move independently of each other. An example of the transformation of the walls to disclinations is shown in Figs.7 and 8. This process has been observed in ordinary low molecular weight nematics[22] and is another example of the similarities between polymer liquid crystals and low molecular weight liquid crystals.
To collect quantitative data on these instabilities, four samples of TMV were prepared with concentration 148 mg/ml in a 50 mM Borate buffer of pH 8.5 and in a cell thickness of 90µm, 201µm, 290µm, and 366µm.

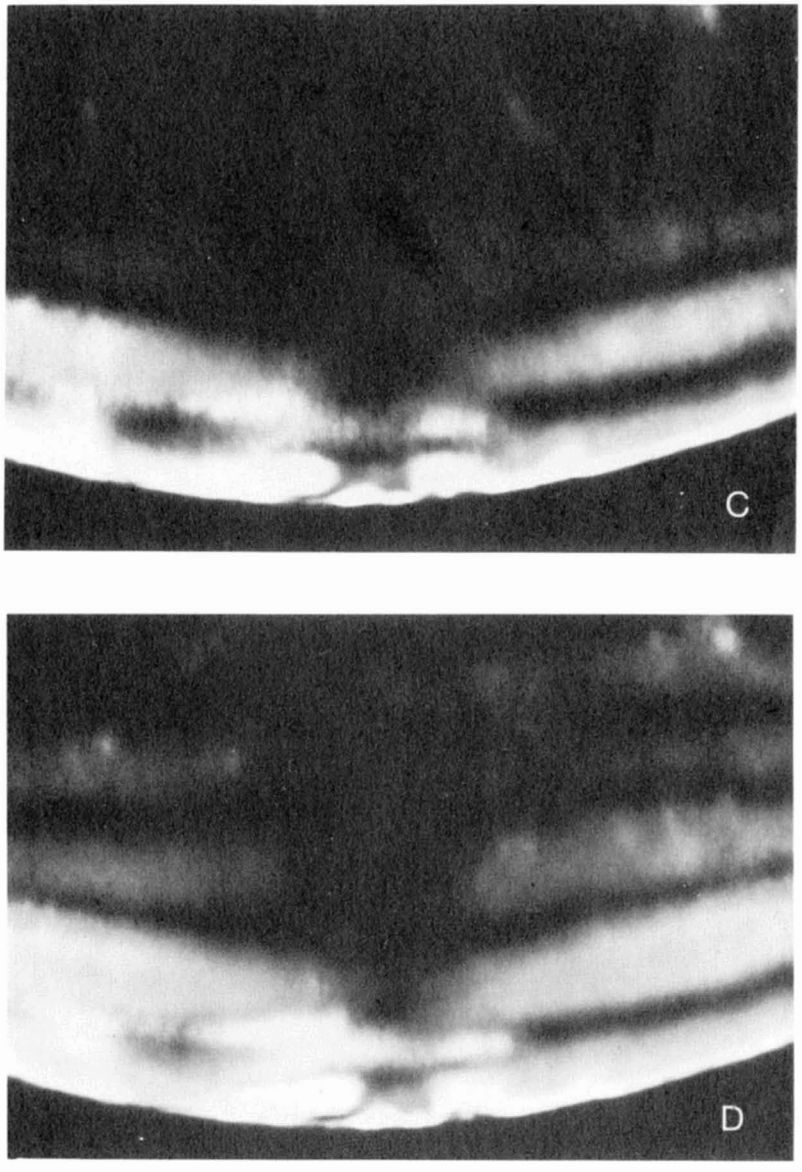

Figure 6C-D

After annealing in a large field to obtain a uniformly aligned sample a cell was exposed to a known field normal to the director but inthe plane of the sample (the twist geometry). The periodicity of the distortion was measured by counting the number of stripes within a measured distance. Measurements were taken in several regions in the sample and averaged. Although the measurements were taken outside of the field, the walls did not relax nor did the wavelength change during the short time the measurement was taken. We studied the periodicity of

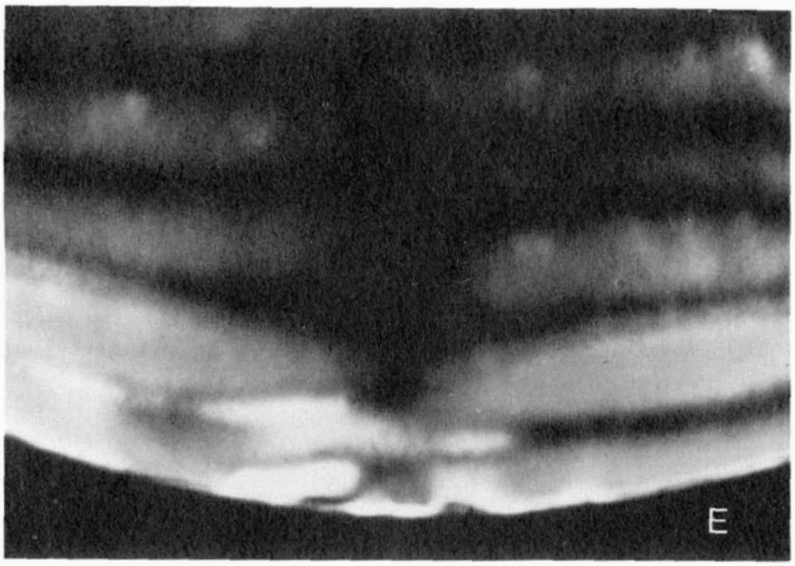

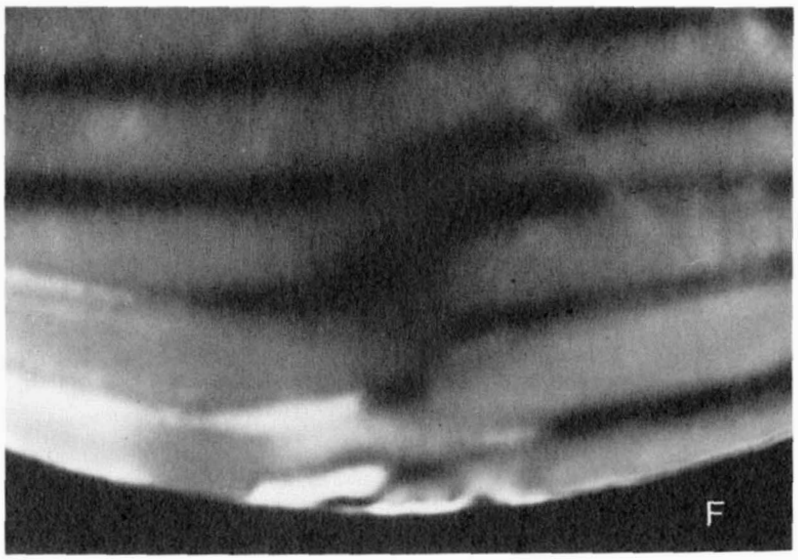

Figure 6E-F

Figure 6 Temporal development of the periodic twist transition

The sample was TMV in water at a concentration of 60 mg/ml in a cell of 400 microns thickness. (A) One minute after a field of 5 kgauss was applied. (B-F) Photograghs were taken approximately 45 s apart. As the instability develops in time regions with the same angle of twist anneal together. All photographs in this paper were taken with crossed polarizers.

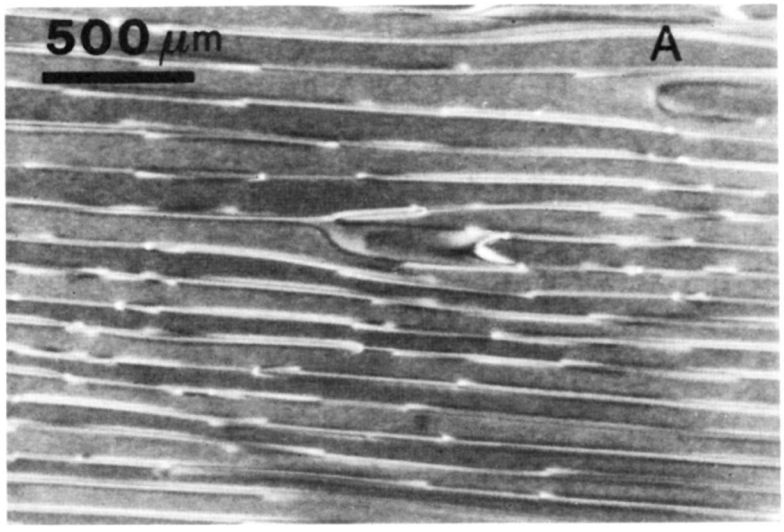

Figure 7A

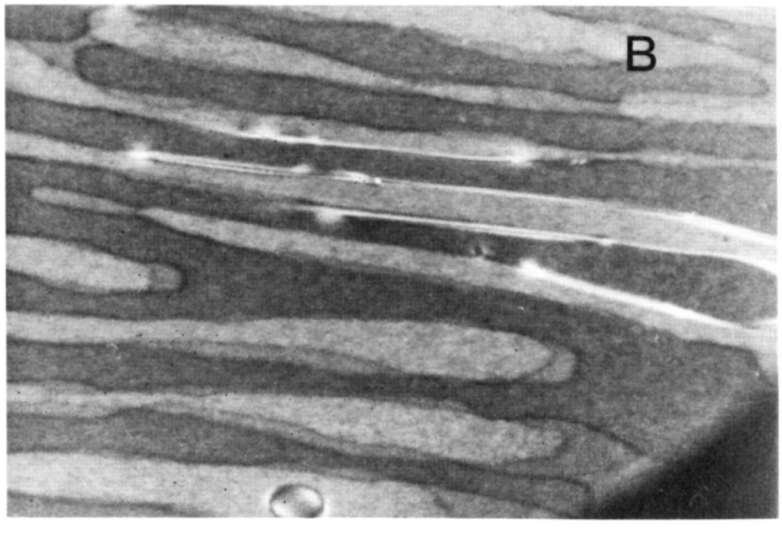

Figure 7B

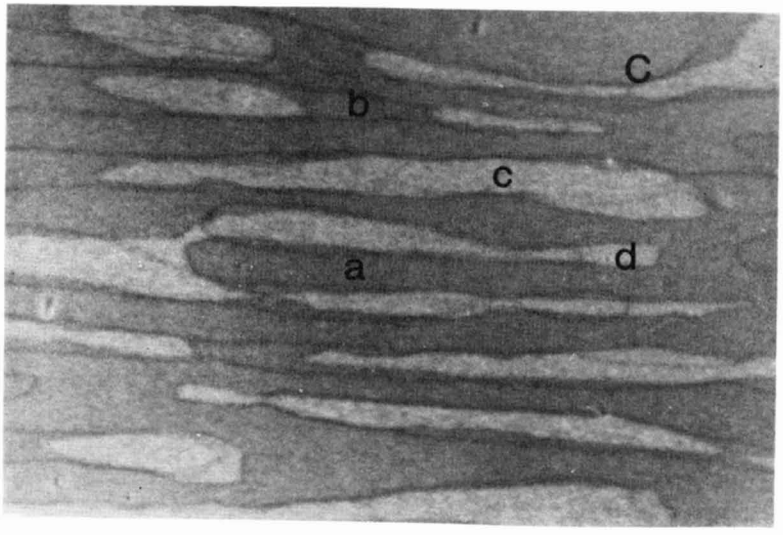

Figure 7C

Figure 7 Twist walls and disclinations formed by the periodic twist transition.

A 297 micron thick sample of TMV nematic of concentration 148 mg/ml, pH 8.5, 50 mM borate buffer in a 15 kgauss field. The samples are photographed with crossed polarizers. (A) Sample has been in the field for five minutes. The polarizer is 45 degrees from the field. The bright lines are twist walls. The director on each side of the wall has twisted in opposite directions but now is parallel to the field which is perpendicular to the walls. The view in this photograph is the same view as in Fig. 5 and a cross-section is shown in Fig. 8A. (B) Same sample as in (A) after one hour in the field. As the sample anneals in a field the twist walls break into disclination pairs. The disclinations have a small core and are very sharply focused. The disclinations formed at a rate of 1 mm/min. The polarizer-analyzer pair has been rotated so it is no longer symmetric with respect to the field. Regions of different sign of twist give birefringence different colors. (See Fig.8B). (C) The four differently colored regions labeled (a-d) correspond to the four possible combinations of twisted material created by independent disclinations (See Fig. 8C).

the instability as a function of the magnetic field strength and sample thickness. The data with a theoretical fit are shown in Fig.9.

The theoretical expression for the rate of growth (s) of the periodic twist transition is[20]

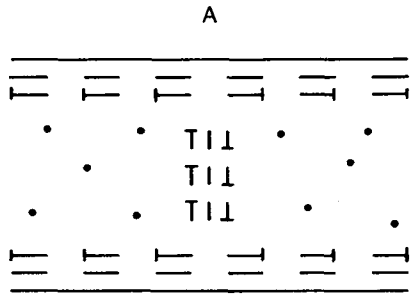

Figure 8A

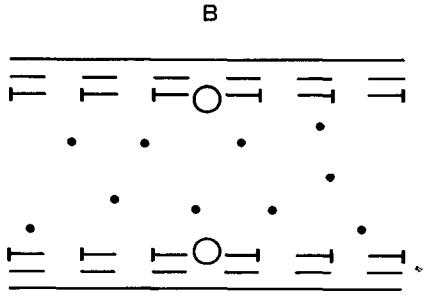

Figure 8B

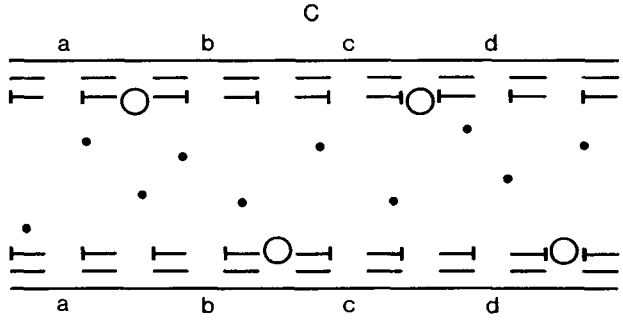

Figure 8C

Figure 8 Twist walls and disclinations formed by the periodic twist transition.

The three drawings here correspond to section views of Figs. A-C. The magnetic field is normal to the page for this figure. The director normal to the page is represented by (o), the director parallel to the page (-), right-handed rotation of the director (⊢—), and left-handed rotation (—⊣). (A) The director pattern of a twist-bend wall. (B) The director pattern of two ±1/2 disclinations which have moved to the cell surface. When the polarizer-analyzer pair is crossed at 90 degrees but not symmetric to the field, the regions of right-handed and left-handed twist will be differently colored. (C) The disclinations have separated. There are shown four regions of different twist labeled a-d corresponding to Fig. 7. In region (a) the director (as followed from bottom to top) first twists to the right then back to the left (RL). In region (b) the director twists RR. In region (c) the director twists LR and in region (d) the director twists LL.

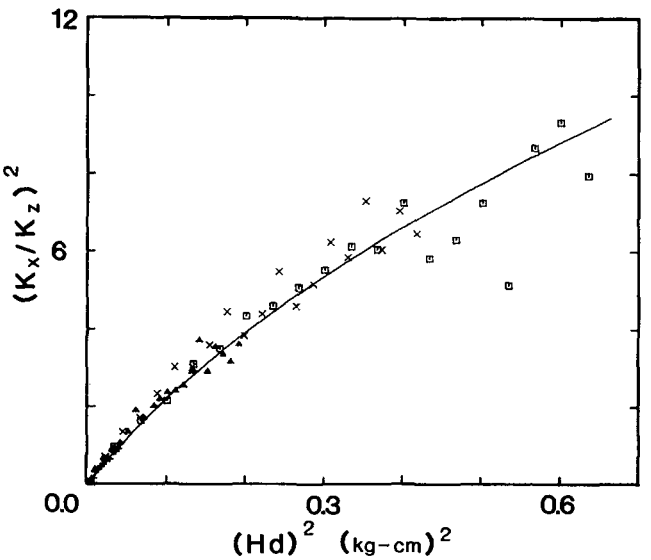

Figure 9 Magnetic field dependence of the wave vectors in the periodic twist transition.

Four samples of different thicknesses from 94-366 microns and fields from 5-22 kgauss were used. All samples contained TMV of 148 mg/ml in pH 8.5 borate buffer. The data are fitted by the theory using a least-squares fit that is constrained to have a threshold of the periodic response at H/Hc=2. The different symbols are for samples of different thicknesses. (+) = 90 μm, (△) = 201 μm, (X) = 297 μm and (□) = 366 μm. The wave vectors are defined as: $k_z = \pi/d$ and $k_x = 2\pi/\lambda$ where λ and d are defined in Fig. 3.

$$s(\text{periodic}) = \frac{\chi_a H^2 - K_2 k_z^2 - K_3 k_x^2}{\gamma_1 - \frac{\alpha_2^2}{\eta_c + \eta_a \left(\frac{k_z}{k_x}\right)^2}} \qquad (1)$$

where H is the magnetic field, χ_a the diamagnetic anisotropy, k_x and k_z wave vectors of the distortion with k_z assumed to be constant at π/d and d the sample thickness. The other coefficients are defined as usual in the literature[23] and characterize the visco-elastic properties of the liquid crystal. As discussed above the wave vector that is observed is the wave vector that has the greatest rate of growth. This is found by maximizing the rate of growth with respect to k_x at a fixed value of H, yielding the following relation:

$$(H/H_c)^2 = \left(\frac{1-\alpha}{\eta\alpha}\kappa\right)x^2 + \left(\frac{2\kappa}{\alpha}\right)x + \left(1 + \frac{\kappa\eta}{\alpha}\right) \qquad (2)$$

where $x = (k_x/k_z)^2$, $H_c = (\pi/d)\sqrt{(K_2/\chi_a)}$, $\alpha = \frac{\alpha_2^2}{\eta_c\gamma_1}$, $\eta = \frac{\eta_a}{\eta_c}$, $\kappa = \frac{K_3}{K_2}$.

We wish to determine when the liquid crystal responds to reorientation by the periodic process. Uniform reorientation involves no flow and the rate is given by[24]

$$s(\text{uniform}) = \left(\left(\frac{H}{H_c}\right)^2 - 1\right)\frac{K_2 k_z^2}{\gamma_1} \qquad (3)$$

We seek the field H where the periodic rate is greater than the uniform rate. Taking the ratio of Eqs.(1) to (3) and substituting in Eq.(2) to eliminate $(H/H_c)^2$ we see that the periodic process occurs whenever

$$(H/H_c)^2 > 1 + \frac{\kappa\eta}{\alpha} = C \qquad (4)$$

Furthermore it can be shown that the initial wavevector k_x is zero when Eq.(4) is satisfied. An upper bound on C was found by measuring the field for which we first observe a periodic response. A lower bound is simply the twist critical field H_c. Using the experimentally measured values of H^2 and x^2 and having bounded C as just described we performed a least-squares fit to the data using Eq.(2). In the fit C was held fixed and the fitting parameters were the coefficients of the linear and quadratic terms in x. We caried C over a reasonable range to investigate how sensitive the fitted visco-elastic parameters are to change in C. For C = 1.5 we found that $\alpha = 0.998$, $k = 43.0$ and $\eta = 0.017$ and for C = 4.0 we found $\alpha = .989$, $\kappa = 41.9$ and $\eta = .071$. It is interesting to compare these visco-elastic parameters with those of a thermotropic liquid crystal. For MBBA the same parameters are[23] $\alpha = .74$, $\kappa = 2,5$ and $\eta = .20$. The TMV values indicate much more anisotropy than the MBBA values in a way that is suggestive of the hard rod[25-28] and infinite chain models[29] which are theories that discuss properties of extremely anisotropic particles like TMV.

Since the duration of the striped metastable structure that arises from a reorientation instability is thousands of times longer with the lyotropic liquid crystals composed of highly elongated particles than with the low molecular weight thermotropics, the instability is easier to observe. The periodic twist Frederiks transition had not been reported in thermotropics like MBBA until recently[20] perhaps because the stripes anneal very rapidly in these liquid crystals and the effect is easily missed if one is not directly looking for it. However the effect is very noticeable in lyotropics and in fact is the dominant response to any rapidly applied reorientating field. We have found experimentally in several lyotropic systems that stripes appear even if the applied reorienting field is not perpendicular to the initial director. The theory of the periodic twist transition presented by Lonberg et.al.[20] was solved only for the case where the magnetic field is perpendicular to the initial director as in the static Frederiks transition, but this perpendicularity does not appear to be crucial.

B. Periodic splay transition

The second instability we studied experimentally and theoretically was the periodic splay transition. An instability in this geometry has been observed and discussed earlier by Guyon, et.al. using very thick samples of MBBA.[18] They observed a system of stripes perpendicular to the initial director. As in the periodic twist transition, this implies that the fluid flows and the director remain in one plane which simplifies the analysis of the problem. However, with TMV we observe stripes oblique to the initial director and applied field. The oblique stripes have been observed in other lyotropics before,[15-19] but never in low molecular weight thermotropics until now. An analysis keeping track of the three-dimensional velocity and director fields has been presented elsewhere.[30] The basic physics is the same as in the periodic twist transition, that is, periodic flow in a certain pattern determined by a combination of anisotropic viscosities and elastic constants maximizes the response rate. The theory predicts that MBBA should produce oblique stripes at low values of the magnetic field and we have observed this experimentally.

The time development of the periodic splay transition instability is very different from the development of the periodic twist transition. The initial appearance of the instability is a diamond lattice of bright and dark spots that nucleate throughout the cell. This lattice is a superposition of two independent periodic distortions where each wave vector is oblique to the original director. The wavelength and the magnitude of the angles of the wave vectors are equal but the angles have opposite sign measured with respect to the original director. As time progresses the dark and light spots connect to form oblique stripes symmetric about the original director. This means that locally one oblique wave vector dominates the other. Between stripes the sample becomes essentially homeotropic (Fig.10).

The time scale for the development of the stripes from the beginning of the transition is of the order of 100 seconds. Once the stripes or splay-bend walls are formed they exist for several hours. As time increases the structures become smoother, and both the angles between stripes and the wavelength increase. The stripes often form closed loops which contract very slowly. After several hours the walls transform into disclination pairs, as in the twist transition. The time evolution of the periodic splay transition is shown in Fig.11.

The oblique stripes can be described by two wave vector components in the plane of the sample (see Figure 4 caption). We measured these wave vector components as a function of the field in the same four samples as in the periodic twist transition measurements. The measurements were made by leaving the samples in the field until the stripes were well formed but before any long term annealing occurred and then placing them under a polarizing microscope and photographing them. Care was taken to photograph the same area in the sample each time. The wavelength and orientation of the stripes relative to the original director was determined. The stripes would relax slightly when taken out of the field but this relaxation amounts to a broadening, not a change in wavelength or angle. The results are plotted in Fig.12 in a way similar to the twist data where, again, k_z is assumed to be π/d. The data plotted in this way should be independent of sample thickness; experimentally we see that they are. It is interesting to note that the reduced wave vector-squared $(k_y/k_z)^2$, approaches the constant 2 independent of the field while $(k_x/k_z)^2$ continues to increase as a function of increasing field. The theoretical fit is from a model that satisfies free boundary conditions while experimentally we have

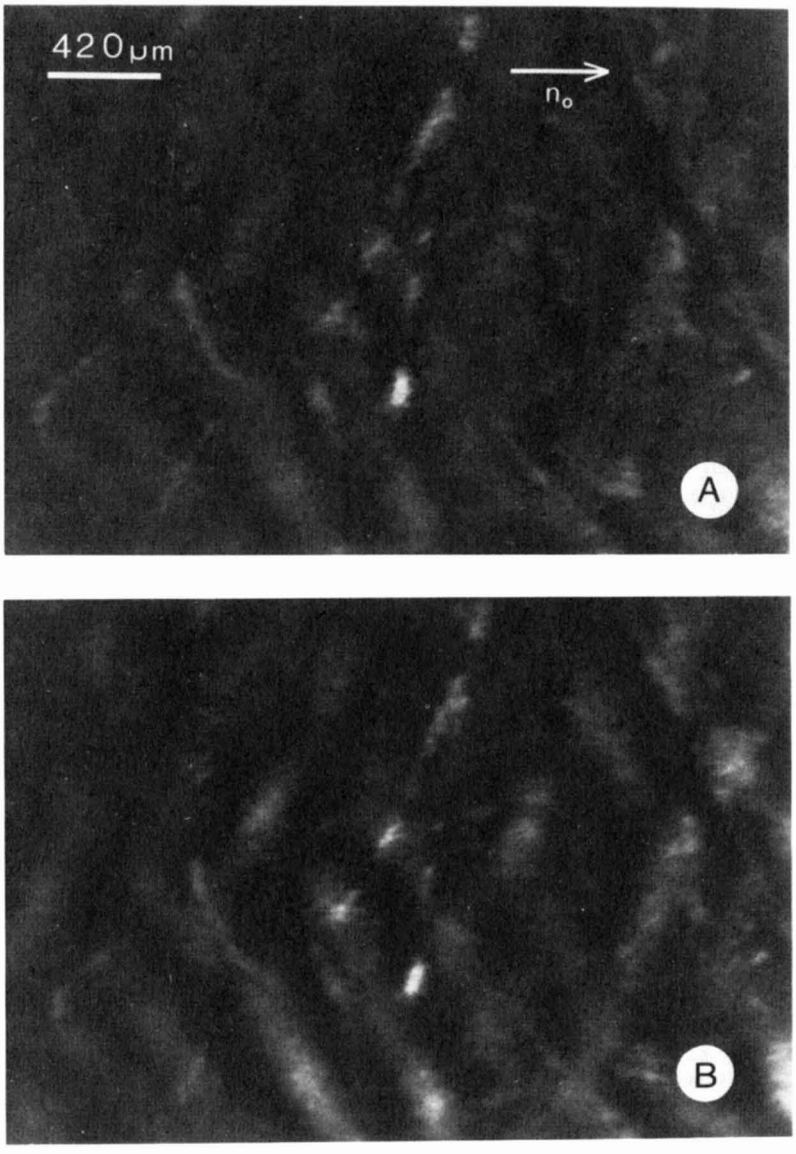

Figure 10A-B

rigid boundaries. The visco-elastic parameters used here are consistent with the parameters used in the periodic twist transition fit. What one sees when looking at these samples under the microscope is that at low fields the stripes have an acute angle (angle θ in Fig.4) with respect to the original director that increases as the field is increased, so that at high fields the stripes are nearly perpendicular to the original director. The wavelength also decreases as the field increases.

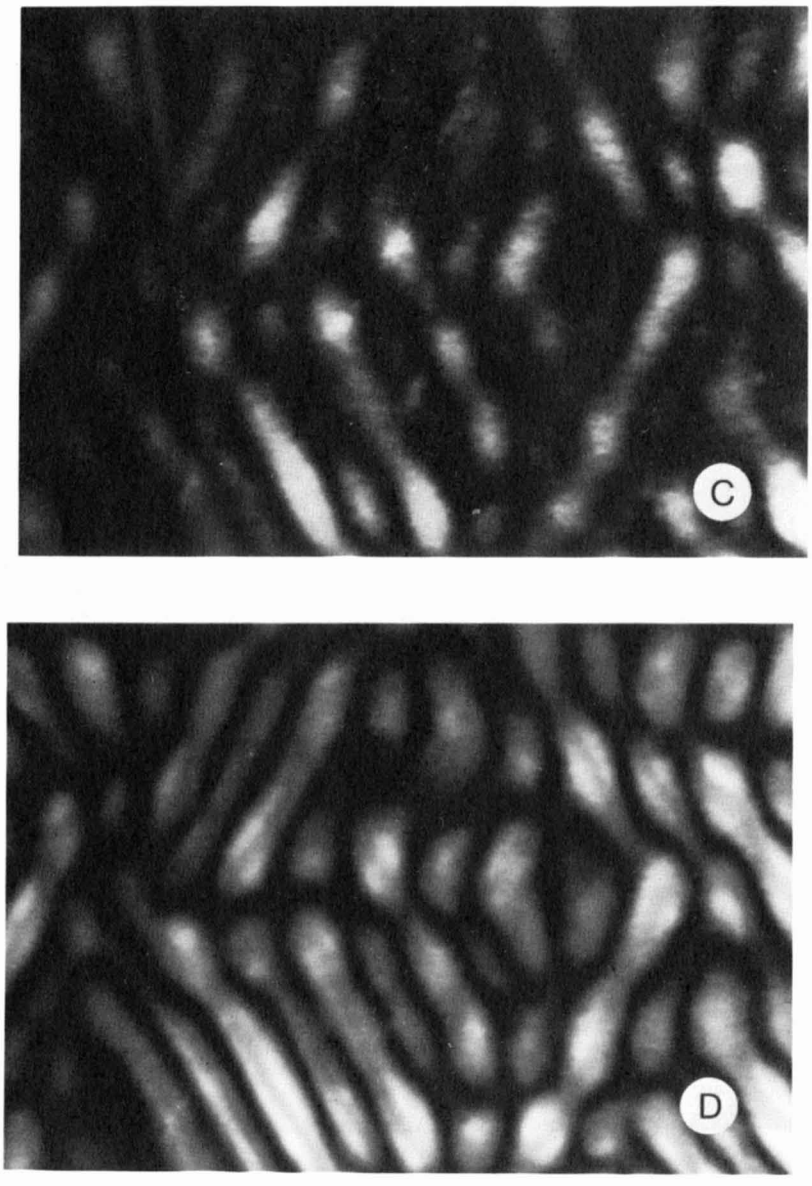

Figure 10C-D

We also made optical Fourier transforms of the photographs of the stripes. The width of the peaks gives an idea of the spread in wavelengths in each experiment. One sometimes observes a weak diffraction peak of twice the wavelength (half the distance to the brightest maximum). This period doubling is due to the pairing of stripes into closed loops - not an approach to chaos. The optical transform of the MBBA sample in the splay periodic transition shows the large degree to

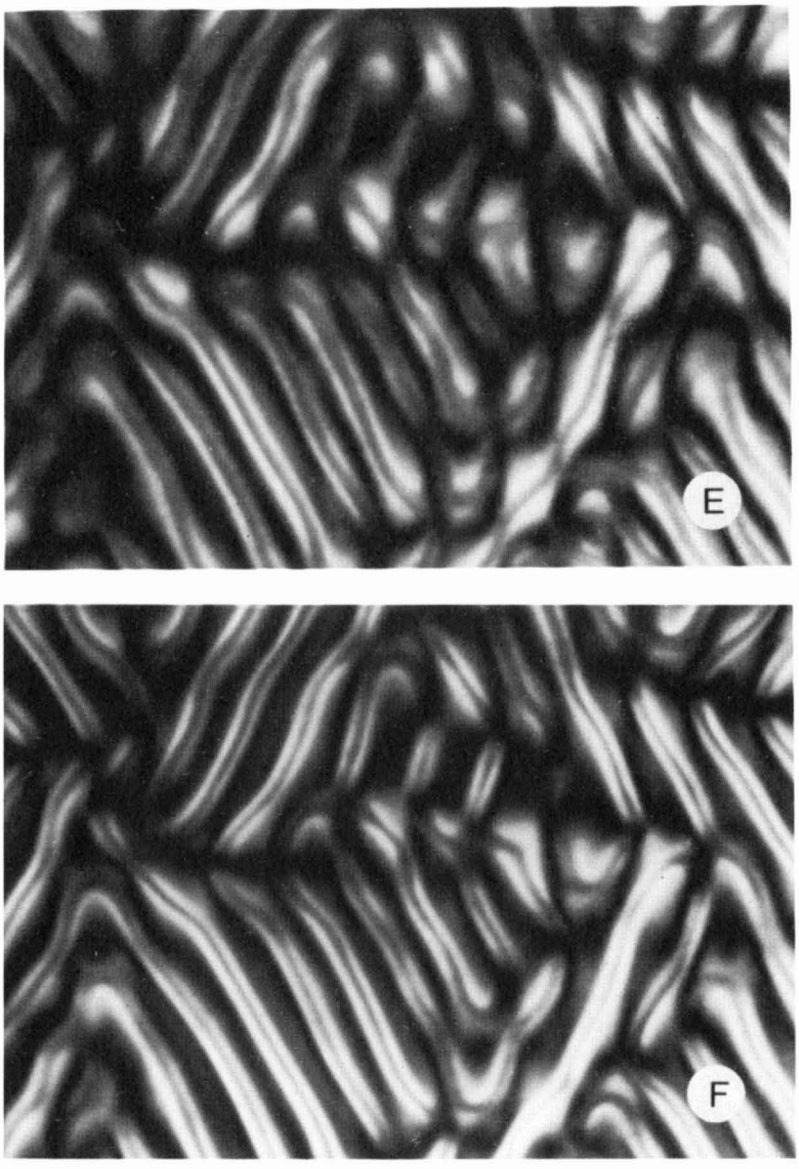

Figure 10E-F

which the pairing of stripes has progressed and the small deviation in the angle of the stripes from being perpendicular to the original director (Fig 13).

To conclude this section on periodic Frederiks instabilities, our experience indicates that the periodic transition is the general response to a rapidly applied reorienting field. This field does not

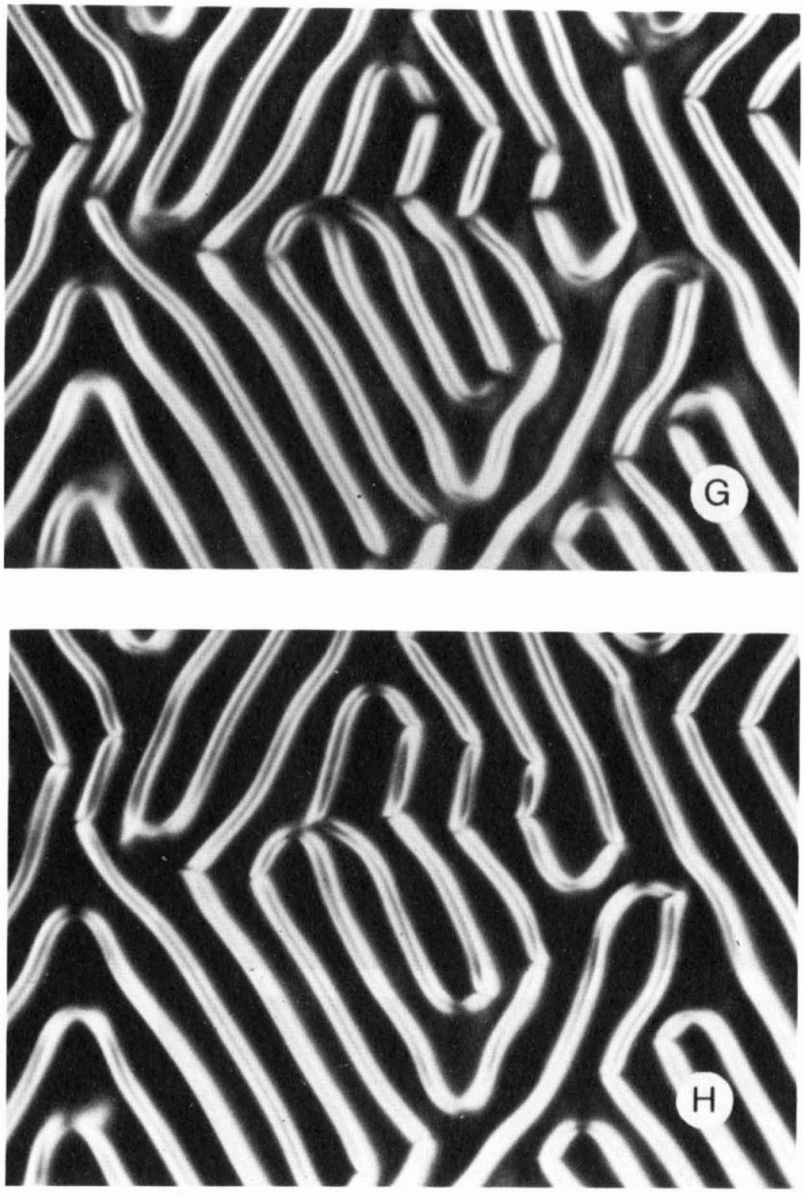

Figure 10G-H

Figure 10 Time development of the periodic splay transition.

The initial response to a suddenly applied magnetic field is a superposition of two wave vectors oblique with respect to the initial director (n) and magnetic field (which is perpendicular to the plane of the page). As the instability develops in time one wavevector dominates in a local domain. The sequence of photographs is for a sample of TMV in water, 60 mg/ml, thickness 400 μm and in a 9 kgauss field. (A-F) are taken approximately at one minute intervals and (G-H) are taken at five minute intervals.

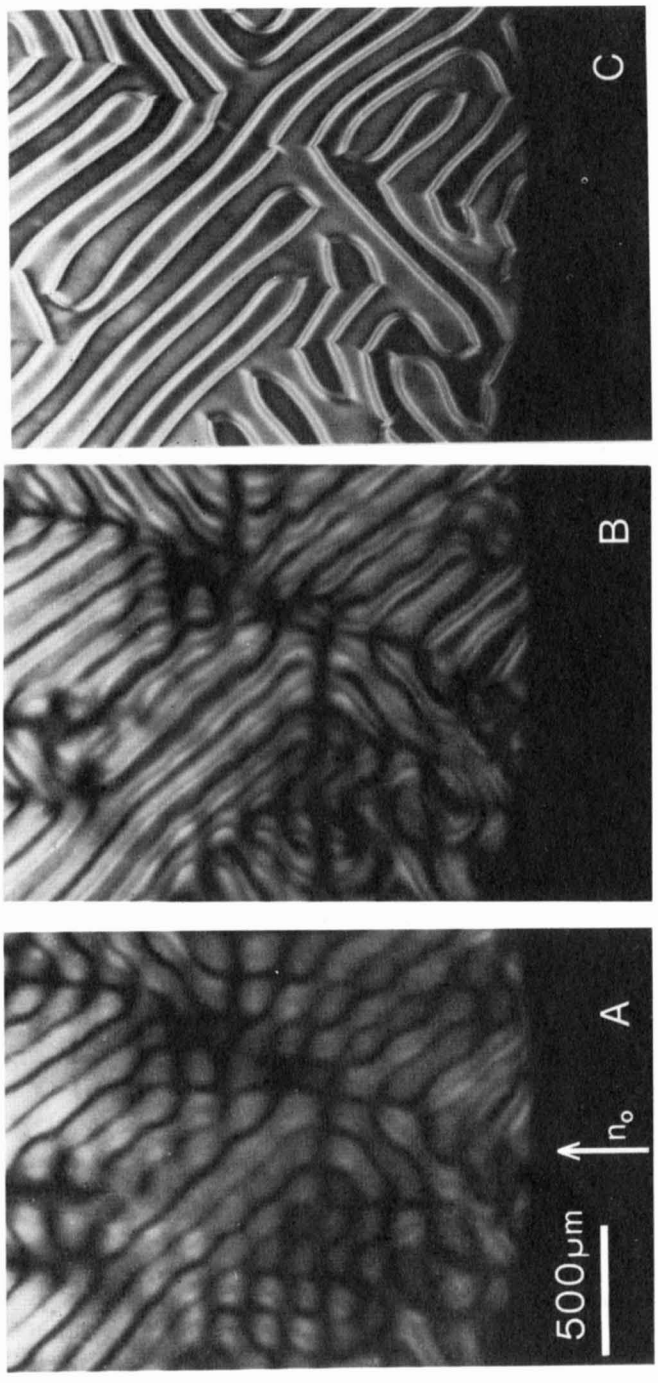

Figure 11A-B-C

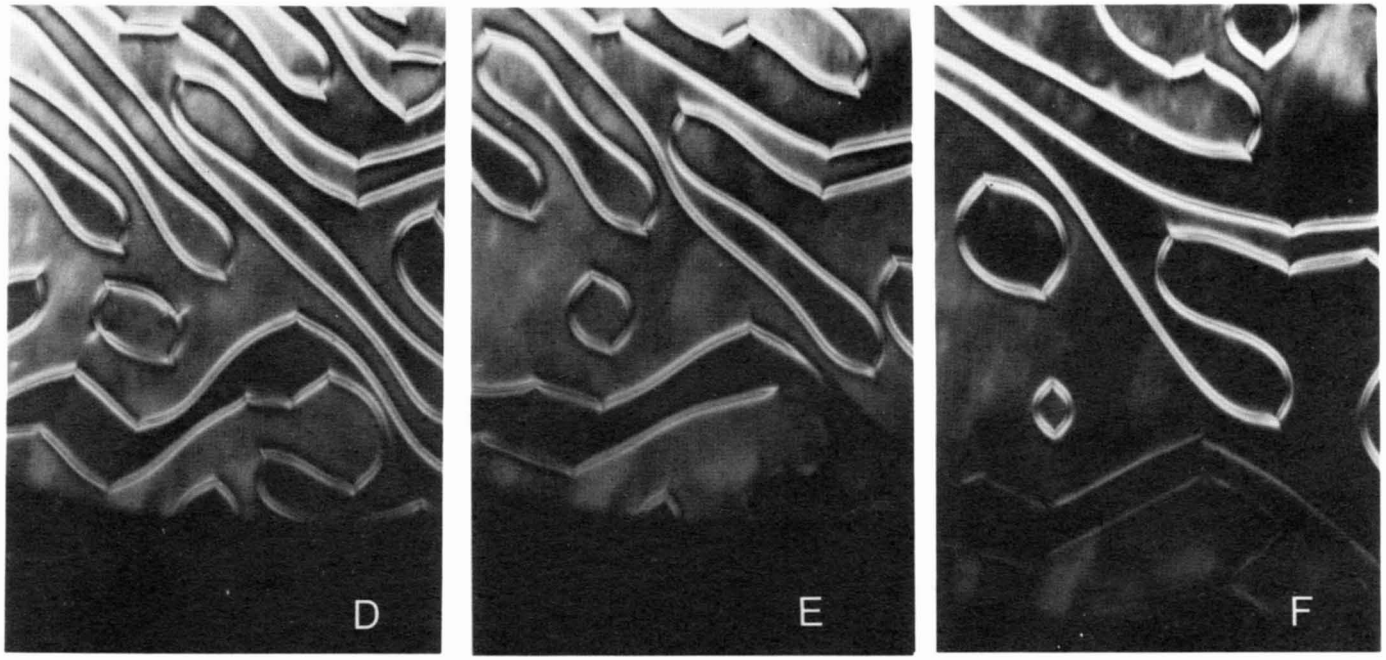

Figure 11D-E-F

Figure 11 Long time behavior of the periodic splay transition.

(A-C) are taken at 90-second intervals and (D-F) are taken at 90-minute intervals. As time progresses the defects become smoother, form loops that annililate and the walls break and transform into disclination pairs. The sample was the 297 μm sample of Fig. 9. The initial director is indicated (n) and the magnetic field is perpendicular to the plane of the page.

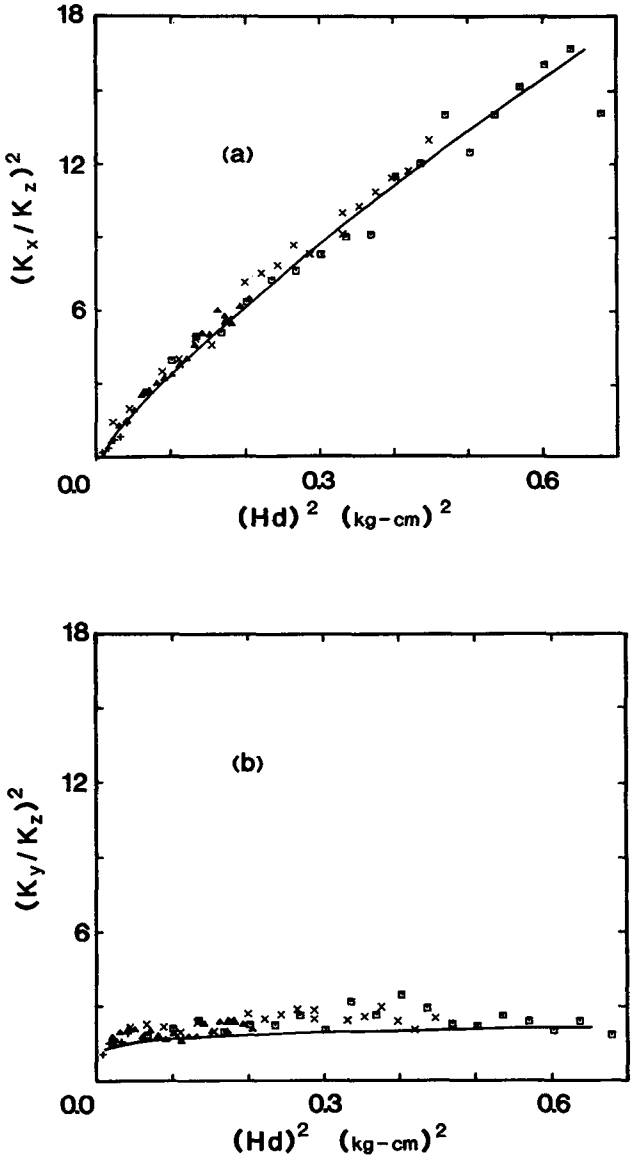

Figure 12 Magnetic field dependence of the wave vectors in the periodic splay transition.

The samples and the field strengths used are the same as in the periodic twist transition. The theoretical fit is to a model that satisfies free boundary conditions while experimentally the boundary conditions are rigid. The visco-elastic parameters used in the fit are the same as in the twist instability. $k_x = 2\pi \sin\theta/\lambda$, $k_y = 2\pi\cos\theta/\lambda$ and $k_z = \pi/d$ where θ, λ, and d are defined in Fig. 4.

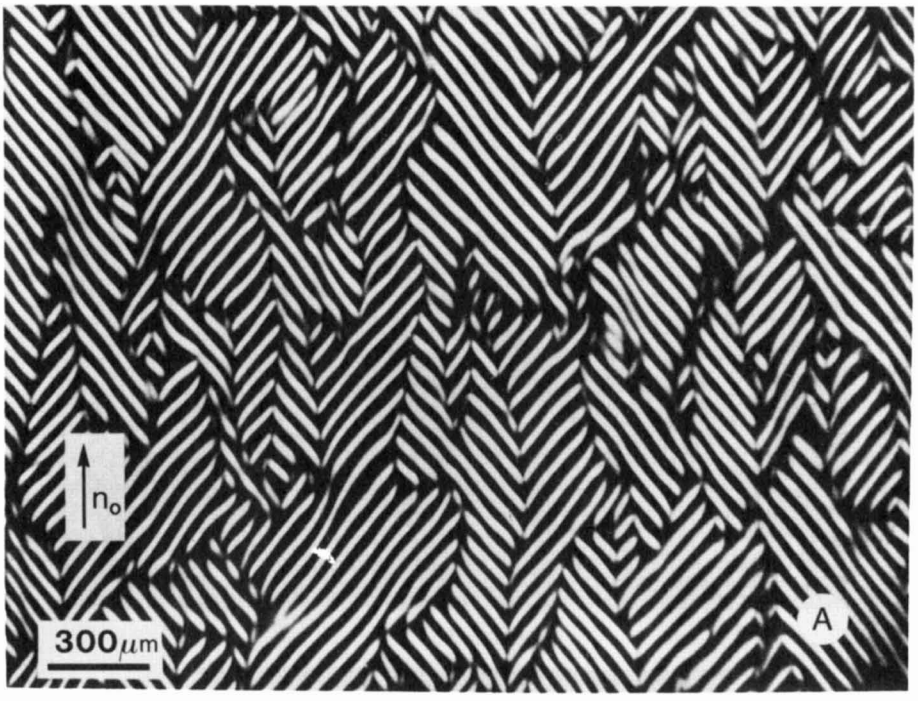

Figure 13A

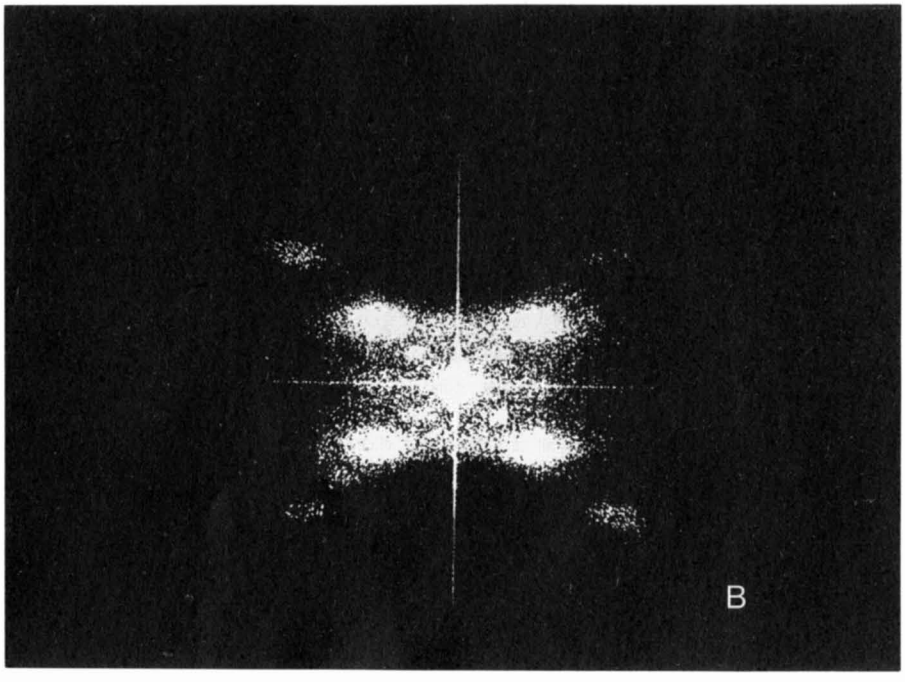

Figure 13B

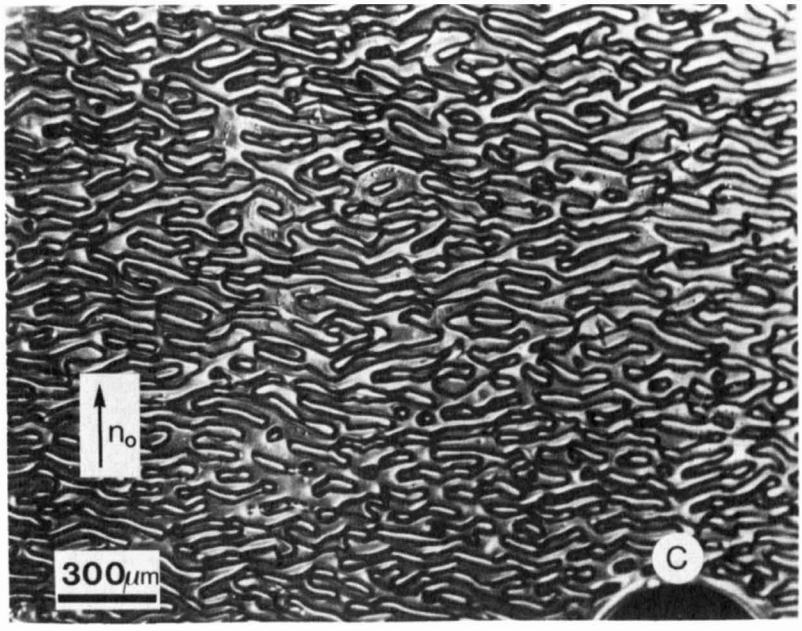

Figure 13C

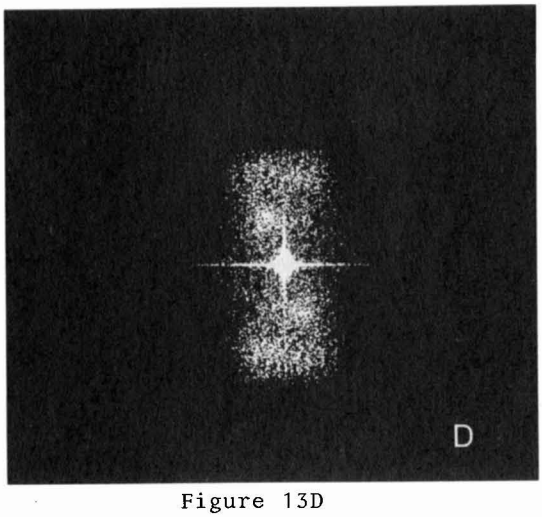

Figure 13D

Figure 13 Periodic splay transition in TMV and MBBA.

(A) The sample is the 90 μm sample of Fig. 9 and $(Hd)^2$ equals 4.1×10^{-2} kg^2 cm^2. (B) Optical Fourier transform of (A). Notice the period doubling. This is caused by pairing of the stripes into loops. (C) MBBA with $(Hd)^2$ equals 2.5×10^{-2} kg^2 cm^2. The instability is short-lived in MBBA and one can see that the sample is annealing towards an aligned homeotropic state. (D) Optical Fourier transform of (C). The large degree of pairing of the stripes is indicated by the intensity of the first and second maxima. The k_y component is much smaller than the k_x component as seen by the small angle subtending the diffraction maxima.

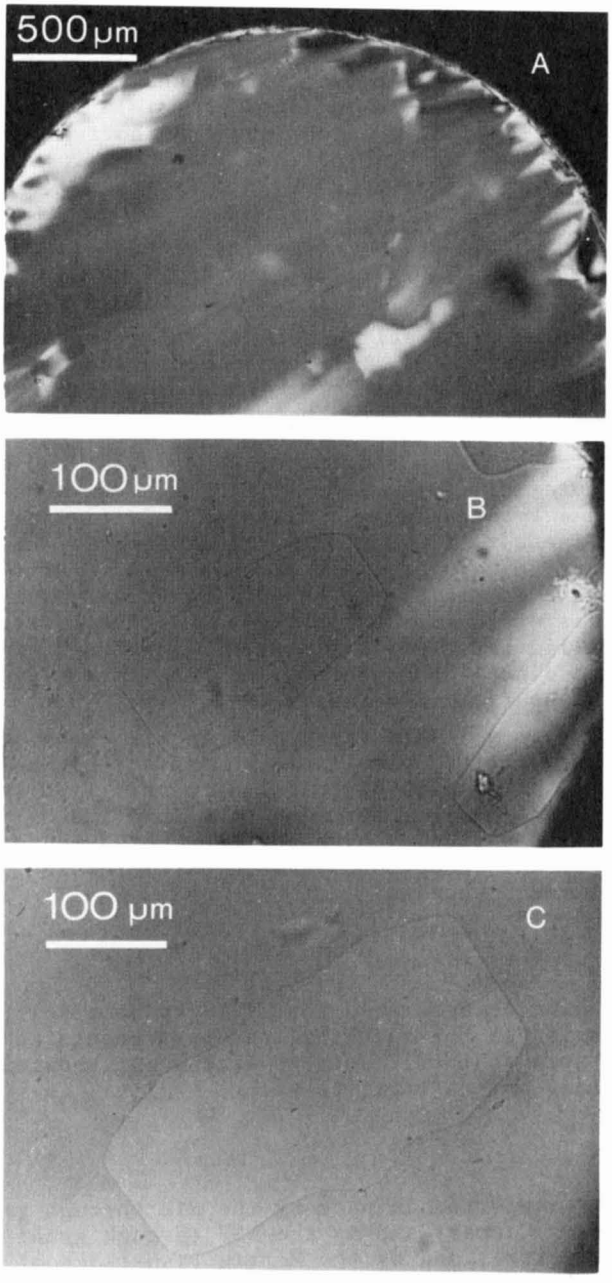

Figure 14 Colloidal crystalline TMV.

This single crystal of TMV was grown over several months in a 4 kgauss magnetic field. The sample is 180 mg/ml of TMV in 50mM borate buffer, pH 8.5 and is placed in a SiO treated cell. The photographs were taken with crossed polarizers.

have to be perpendicular to the original director for the effect to occur. The effect is not easily seen in low molecular weight thermotropics because the defects formed by the instability anneal quite rapidly. However, the periodic Frederiks transition is the dominant response to a reorienting field in liquid crystals composed of long particles. This distinction between long and short particle nematics at a microscopic level is reflected in differences in their marcoscopic visco-elastic properties.

5. COLLOIDAL CRYSTALLINE TMV

It has been reported that TMV will form colloidal crystals in distilled water at concentrations of 25 mg/ml and above.[5,7] These authors report that the addition of salt dissolves the crystals and, depending on how much salt is added, the sample becomes nematic or isotropic or it aggregates and precipitates. However, we have formed colloidal crystalline TMV in buffered borate solutions of pH 8.5 with an ionic strength of 10-50 mM. We found that with these conditions colloidal crystals form at a concentration of about 160 mg/ml. We placed this material in a cell with SiO treated windows and placed the cell in a 4 kgauss field to align it. Initially the sample was polycrystalline but it eventually was aligned by the field and surfaces. No large single crystals were observed. After about one month larger single crystals grew out of the polycrystalline region with the long axis of the crystal along the director; these crystals are shown in Fig.14. The sample gives brillant Bragg reflection of light in a single direction demonstrating that the Bragg planes are perpendicular to the field and sample windows.

Single crystal TMV is suitable for quasi-elastic light scattering studies to explore lattice dynamics in an anisotropic colloidal crystal. The dynamics and statics of colloidal crystalline TMV could be explored by light and X-ray scattering as a function of pH and ionic strength. Since these studies have not been performed on colloidal crystals formed of anisotropic rod-shaped particles they would undoubtedly reveal new phenomena.

6. CONCLUSIONS

We hope that we have demonstrated that TMV can be a well characterized liquid crystal suitable for quantitative measurements and that it will prove to be a system that will help to extend our knowledge of the nematic and colloidal crystalline states.

ACKNOWLEDGEMENTS

This research was supported in part by the NIH through grant no. CA 15468 (to D.L.D. Caspar) and by the NSF through grant no. DMR-8210477 (to R.B. Meyer), and by the Martin Fisher School of Physics and the Rosenstiel Basic Medical Science Research Center of Brandeis University.
We benefited from useful discussions with Professor Henk Lekkerkerker of the Vrije Universiteit Brussel and with Dr. Michael Cross of AT&T Bell Laboratories.

REFERENCES

1. D.L.D. Caspar, Advan.Protein Chem.18, 37, (1963)
2. S. M. Ahmed, M. S. El-Asser, G. H. Pauli, G. W. Poehlein, and J. W. Vanderhoff, J. Coll. Interface Sci.73, 388, 1980
3. H. Boedtker and N. S. Simmons, J. Amer. Chem.Soc.80, 2550, (1958).
4. J. Gregory and K. C. Holmes, J. Mol.Biol.13, 796, (1965)
5. U. Kreibig and C. Wetter, Z. Naturforsch.35c, 750, (1980)
6. G. Maret, S. Fraden, R. B. Meyer and D.L.D. Caspar, unpublished. We determined the anisotropy of the diamagnetic susceptibility per particle of TMV to be 1.3 x 10^{-25} erg-gauss^{-2}.
7. G. Oster, J. Gen.Physiol.33, 445,(1950)
8. W. M. Stanley, Science 81, 644, (1935)
9. F. C. Bawden, N. W. Pirie, J. D. Bernal and I. Fankuchen, Nature 138, 1051, (1936)
10. J. D. Bernal and I. Fankuchen, J. Gen.Physiol.25,111,(1941)
11. R. J. Best, J. Aust. Inst. of Agric.Sci.5, 94,(1938)
12. L. Onsager, Ann. N.Y. Acad.Sci.51, 627, (1949)
13. P. A. Forsyth, P. A. Marcelja, S. Mitchell Jr. and B. W. Ninham, Adv.Coll. and Interfac. Sci.9, 37, (1978).
14. T. A. Cross, S. J. Opella, G. Stubbs, and D.L. D. Caspar, J. Mol. Biol.170, 1037, (1983)
15. L. J. Yu and A. Saupe, J. Am.Chem.Soc. 102, 4879, (1980)
16. J. Charvolin and Y. Hendrikx, J.Phys.(Paris) Lett. L41, 597, (1980)
17. H. Lee and M. M. Labes, Mol. Cryst.Liq.Cryst.54, 261,(1979)
18. E. Guyon, R. Meyer,and J. Salan, Mol.Cryst.Liq.Cryst.54, 261,(1979)
19. E. F. Carr, Mol.Cryst.Liq.Cryst.34L, 159, (1977)
20. F. Lonberg, S. Fraden, A. J. Hurd,and R. B. Meyer, Phys.Rev.Letts. 52, 1903 (1984).
21. G. Dee and J. S. Langer, Phys.Rev.Lett.50, 383 (1983); G. Ahlers and D. S. Cannell, Phys.Rev.Lett.50, 1583 (1983); E. Ben-Jacob, H. Brand, G. Dee, L. Kramer and J. S. Langer, Physica D, to be published
22. P. G. Gennes, Physics of Liquid Crystals, Sec.4.4.3 (Clarendon Press, Oxford, 1975)
23. Ibid., Chaps.3 and 5
24. P. Pieranski, F. Brochard and E. Guyon, J. Phys.(Paris)34, 35 (1973)
25. J. P. Straley, Phys.Rev.A 8, 2181, (1973)
26. M. Doi, J. Polymer Sci.19, 229, (1981)
27. M. Doi, Ferroelectrics 30, 247, (1980)
28. G. Marruci, J. Mol.Cryst.Liq.Cryst.72L, 153L, (1982)
29. R. B. Meyer in "Polymer Liquid Crystals", edited by A. Ciferri, W. R. Kribaum, and R. B. Meyer, Chap.6, (Academic Press, New York 1982)
30. A. J. Hurd, S. Fraden, F. Lonberg and R. B. Meyer, J.Phys.(Paris), in preparation.